Experimental and numerical analyses of full-span floors and component level subassemblies for robust design of CLT floors

Experimental and numerical analyses of full-span floors and component level subassemblies for robust design of CLT floors

Alicja Przystup, PhD candidate, School of Engineering, University of Edinburgh, United Kingdom

Thomas Reynolds, Lecturer, School of Engineering, United Kingdom

Thomas Tannert, Professor, School of Engineering, University of Northern British Columbia, Canada

Keywords: Robustness, progressive collapse, catenary action, combined loading

1 Introduction

1.1 Robustness of tall timber structures

Tall mass timber structures are becoming increasingly prevalent and, with some now rising as tall as 81m (Abrahamsen, 2017) it is vital to consider design for structural robustness and disproportionate and progressive collapse prevention under accidental actions (Starossek & Haberland, 2012). The Eurocode 1-7 approach (European Committee for Standardization, 2006) focuses on material independent objective-based design. An inherent robustness through alternative load paths (ALPs), primarily catenary action, is targeted through introduction of vertical and horizontal ties. This is a prescriptive approach without the necessary physical basis when introducing novel construction methods.

Previous experimental work on catenary action in mass timber floors, specifically floors made of cross-laminated timber (CLT) (Lyu et al., 2020; Mpidi Bita & Tannert, 2019) suggested that common connections designed to current standard requirements might not be appropriate for sufficient load redistribution to develop catenary action due to their limited deformation capacity. Performance-based design methods such as the robustness index method (Voulpiotis et al., 2021) have been proposed to capture the physical behaviour of the system, but such methods require experimental research to provide the necessary input parameters.

1.2 Connection properties under catenary action

After the loss of a load-bearing member, a crucial mechanism called catenary action comes into play, allowing for the redistribution of load within the structure. A common scenario where this mechanism occurs is when two floor panels are joined over a support, and that support is lost, as depicted in Figure 1. Under catenary action, the floors, which typically endure bending and shear forces, experience a combination of bending and tension. Understanding the effect of this combined loading on mass timber connections is essential for effective modelling and performance-based design.

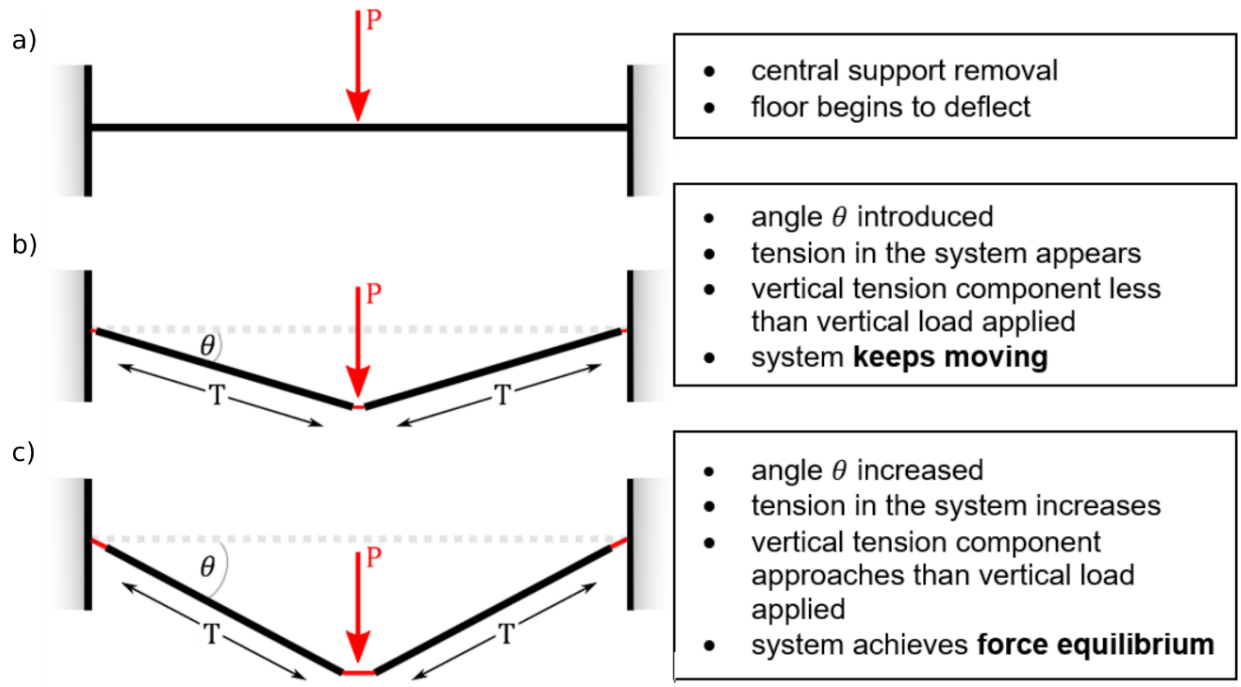

Figure 1: The progression of catenary action in a floor with a joint at mid-span

The required parameters to accurately predict the second-order deformation behaviour of such floor-to-floor subassembly are: i) rotational and axial stiffnesses of connection and supports, ii) maximum rotation of central connection, and iii) maximum axial displacement of central connection. The main challenges to develop catenary behaviour in timber structural systems are the lack of reliable plastic deformations within the timber and connections, and the orthotropic nature of the material. The interaction of these parameters with one another influences the loads within this system (pictured in Figure 2) and can only be predicted and with empirical evidence.

Initially, the magnitude of the vertical load defines the angle of rotation and the tension demand, as shown in Figure 1a. The tension demand decreases with increasing angle of rotation (Figure 1b). The latter affects the rotational stiffness, the value of which affects the ability to develop large deformations beyond the elastic limit. Larger axial stiffnesses of connection and support increase the tension demand and ultimately might cause connection failure before catenary equilibrium is achieved (Figure 1c). The angle of rotation and axial stiffness jointly influence the maximum tension developed

in the system. This results in the total horizontal elongation for a given rotation to be achieved. Additionally, the connection tension capacity directly restricts the tension level the system can achieve.

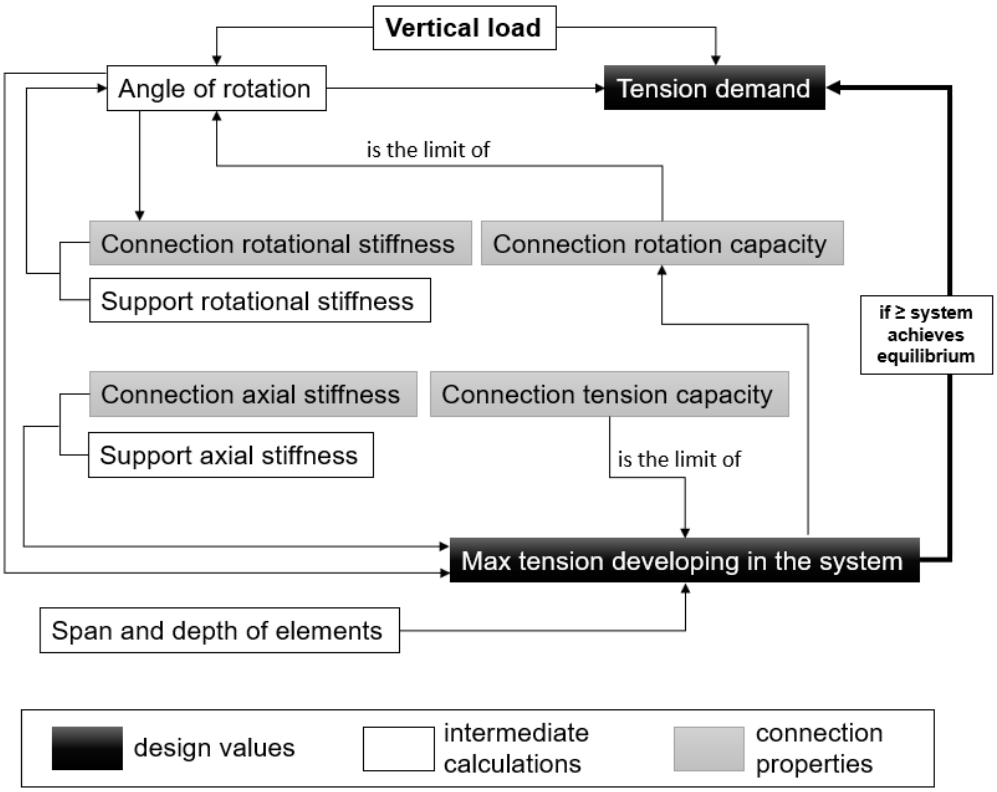

Figure 2: Catenary action parameter interaction diagram

1.3 Objectives

The aim of the research presented in this paper was to conduct an experimental investigation into the mechanical properties of typical floor panel-to-panel Cross Laminated Timber (CLT) connections and floor systems when subjected to combined bending and tension. A secondary objective was to numerically evaluate the potential to predict the full-span test results based on significantly faster and more cost-effective component-level tests. Such experiments are necessary for verification of the objective-based design assumptions. Distilling moment rotation behaviour from simple assemblies can be utilised in performance-based design for defining connector stiffness, strength, and deformation capacity.

2 Experimental investigations

2.1 Materials

CLT panels used in Setup A were produced by the Construction Scotland Innovation Centre to order and had two different panel layups. The 5-ply setup consisted of 20-20-20-20-20mm panels, and the 3-ply setup consisted of 33-34-33mm panels, both with the total thickness of 100mm, with moisture content averaging 9.8%. The CLT

panels used for tests in Setup B were 5-ply 100 mm thick Binderholz BBS 125 of 20-20-20-20-20 mm layer thickness and 10% moisture content.

The tested connections are illustrated in Figure 3. Setup A was used for two series of half lap connections, using a single self-tapping screw (STS) installed at 90-degree without predrilling. The difference between the two series was the panel layup, with the first series using the 5-ply and the second using 3-ply. Setup B was used to test two types of joints using the same CLT panels: spline joints and butt joints. Spline joints used 8x100 mm STS installed through the plywood perpendicular to the surface.

For the butt joints, 8x140 mm STS were installed at 45° at symmetric spacing. The specimens had a width of d = 400 mm and screw spacings of a = 110 mm, b = 100 mm, and c = 90 mm. This butt joint connection was also tested in full span where test specimens had a width d = 600 mm and either 4 or 6 screws with spacings of a = 130 mm, b = 260 mm, and c = 110 mm.

In total 74 component-level specimen were tested with 3 connection types: i) spline joints; ii) half laps with screws in shear, and iii) butt joints with screws in withdrawal. Subsequently, 20 of the full-span specimens were tested under constant tension of 15 kN and 30 kN, and under fixed horizontal displacement with tension increasing as catenary action progressed.

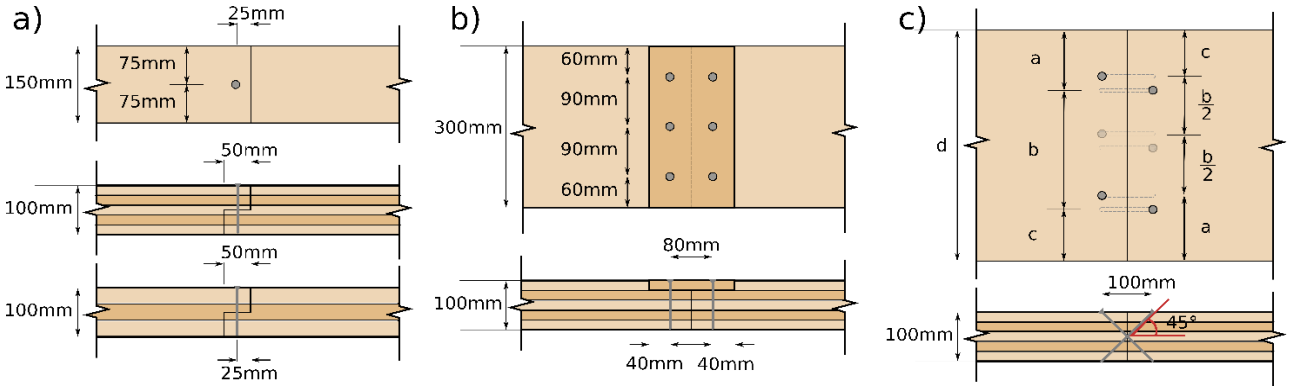

Figure 3: Joint types: a) half lap joint; b) single surface spline; c) butt joint

2.2 Experimental setup

Two types of tests were performed, component and full-span floors, as illustrated in Figure 4a) and b), respectively. Both setup A and B were used for the isolated component-level experiments, with setup B span L = 0.8m. The full-span tests were performed in setup B, where the span L = 3m. The component test was developed for span reduction in combined axial and bending loads, allowing for increased number of tests thanks to the reduction in the volume of timber used per test.

To adequately represent the combined loading condition under catenary action and to be able to be enable comparing the results to the full-span tests, several features were implemented. These features were: i) active application of a secondary horizontal load allowing for any desired level of horizontal tensile load irrespective of setup geometry

and stiffness; and ii) the elimination of compressive arching. Previous research on catenary action utilised some level of physical horizontal restraint at the supports fitted with load cells to impose and measure tension in the system. This only allows for one tension-moment combination at failure to be investigated, governed by the arbitrary stiffness of supports and geometry of the experiment. By introducing an active horizontal loading, any combinations of loads can be implemented on both test scales.

Moreover, compressive arching becomes more significant with an increase in depth-to-span ratio. Using the active load application combined with roller supports which do not restrain the outward movement, allowed for this effect to be minimised to negligible system friction. Therefore, the investigation could focus on extreme rotations and deformations and their effect on the component performance.

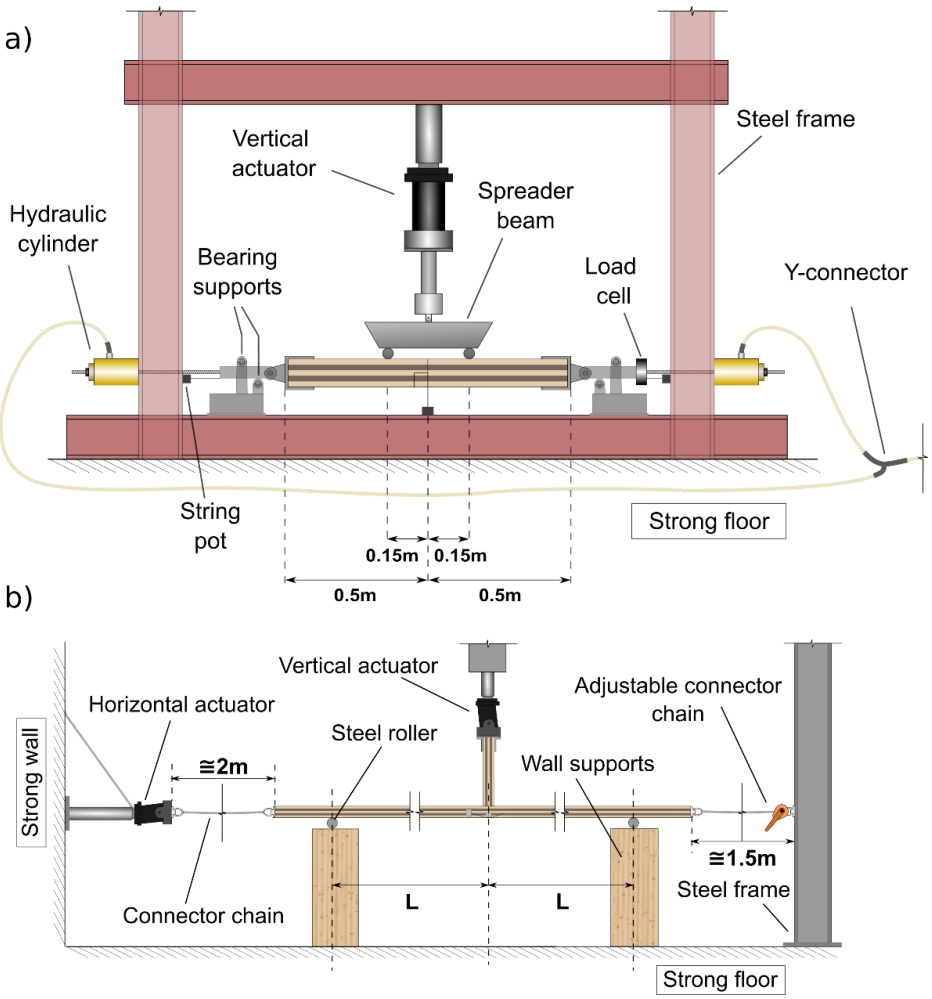

Figure 4: Component test experimental setup A (a) and setup B (b)

2.3 Interaction of applied and internal forces

To determine bending moment capacity, a common approach is 4-point bending, which creates a shear force free zone between the loading points and enables behaviour of the connection to be isolated without additional interaction with the above wall/column element. In building systems however, point loads are often present due to the wall/column acting as the primary load path for vertical loads and therefore a 3-

point bending test is also a useful experimental tool for investigation of connection behaviour with this additional interaction. Both approaches are visualised in Figure 5.

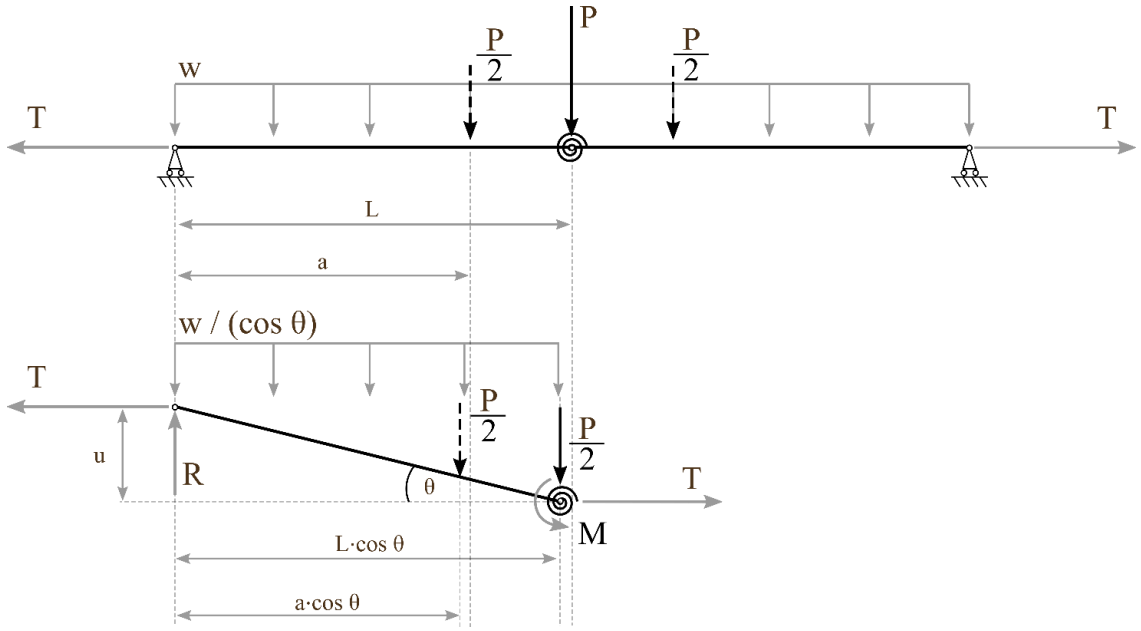

Figure 5: Free body diagrams for 3-point bending (force shown as solid line) and 4-point bending (force shown as dashed line)

In a floor assembly with pin supports and a joint at the centre, when the panel's bending stiffness is significantly higher than the connections', panel deflection is minimal and rotational rigid body movement can be assumed. Equation (1) allows computing the moment at the connection for 4- and 3-point bending (Setup A and B, respectively):

$$M = \frac{(Pa+wL^2)\ cos\,\theta}{2} - T \cdot u \qquad (1)$$

Where P is the central pushdown load, a is the location of load (equal to span L for the three-point bending value of force lever arm), w is the gravity loading of the floors, θ is the angle or rotation, T represents the tension applied to the connection, and u is vertical displacement at midspan.

The tension utilisation T_u of the connection is the ratio of applied tension load T and the connection axial tension capacity the connection (not under combined loading), see Equation (2). It is crucial to highlight that T_u refers to the tension force between the ends of the component and does not represent the fastener utilisation.

$$T_u = \frac{T}{T_{max}} \qquad (2)$$

A 2D-beam model pictured in Figure 5 shows an equal tension T propagated throughout the entire subassembly. One of the important concepts to understand under the combined loading is that in connections (such as butt joints) where a substantial lever

arm generates rotational stiffness, there will be an important differentiation between the applied tension load (T_a) and internal connection tension (T_c).

It is possible to predict the value of T_c through analysing a component as a 3D element, as shown in Figure 6 resulting in Equation (3). In this joint, under combined loading and given significant fastener axial stiffness, the internal resultant tension at the connection T_c will quickly become larger than the applied load T_a, and therefore it will be the value dictating the ultimate strength of the subassembly.

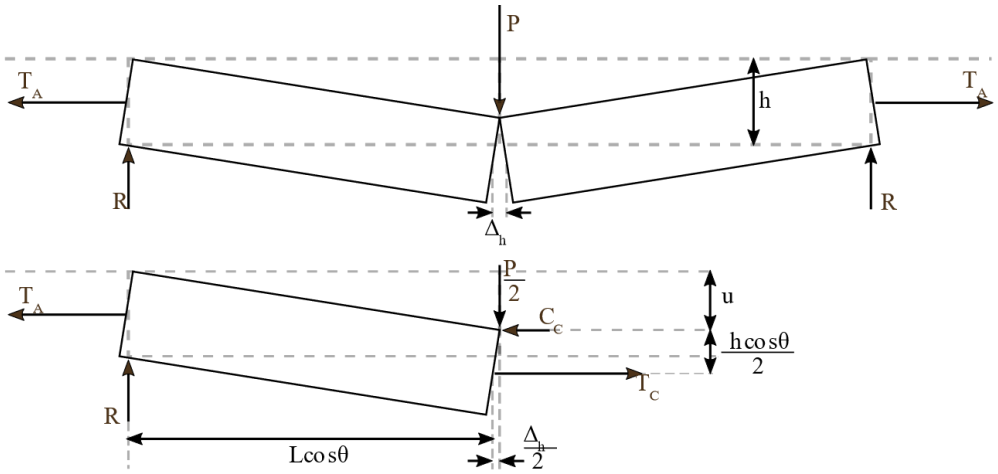

Figure 6: Free body diagram of a butt-joint connection illustrating resultant tension

$$T_c = P \cdot \frac{L}{h} + T_A \cdot \left(1 - \frac{2u}{h}\right) \quad (3)$$

As this relationship is not as straightforward for other joints, an objective measure such as tension utilisation T_u is extremely useful to allow for adequate comparison of moment and rotation capacity under combined loading.

2.4 Results

2.4.1 Influence of tension utilisation on joint performance

The influence of the tension utilisation on the moment and rotation capacity of the connections was evaluated. Figure 7 shows the interaction diagram of the moment tension for all tested connections, and Figures 8 shows the maximum rotation and tension utilisation interaction diagrams. For each test series, 95% confidence intervals (CI) were calculated based on the Extreme Value Distribution Type I (Gumbel, 1948), to account for asymptotic behaviour of the upper outliers of the datasets.

The half-lap and the butt joints showed an inversely proportional relationship of the moment capacity and tension utilisation due to the direct increase of the resultant tension through increased bending. The 5-ply half-lap joint (Figure 7a) and butt joint (Figure 7c) showed an almost perfectly linear relationship, while half-laps in 3-ply test (Figure 7b) showed a decrease of about 25% in its moment capacity until 60% utilisation, with sharp drop off after that point, attributed to splitting failure occurring in the

transverse layer of the 3-ply panels. In contrast, the spline connection (Figure 7d) exhibited an increase in moment capacity up until about 50% T_u, with steep drop off after that point. The interaction in this connection cannot be simplified down to two resultant point loads but is directly caused by the bending and splitting of the plywood. The capacity increase may be attributed to the direct interaction between the wall-stub point load and the spline. Catenary action enables greater overall force and rotation, facilitating sufficient friction between the wall stub and the connection to transfer compressive loads.

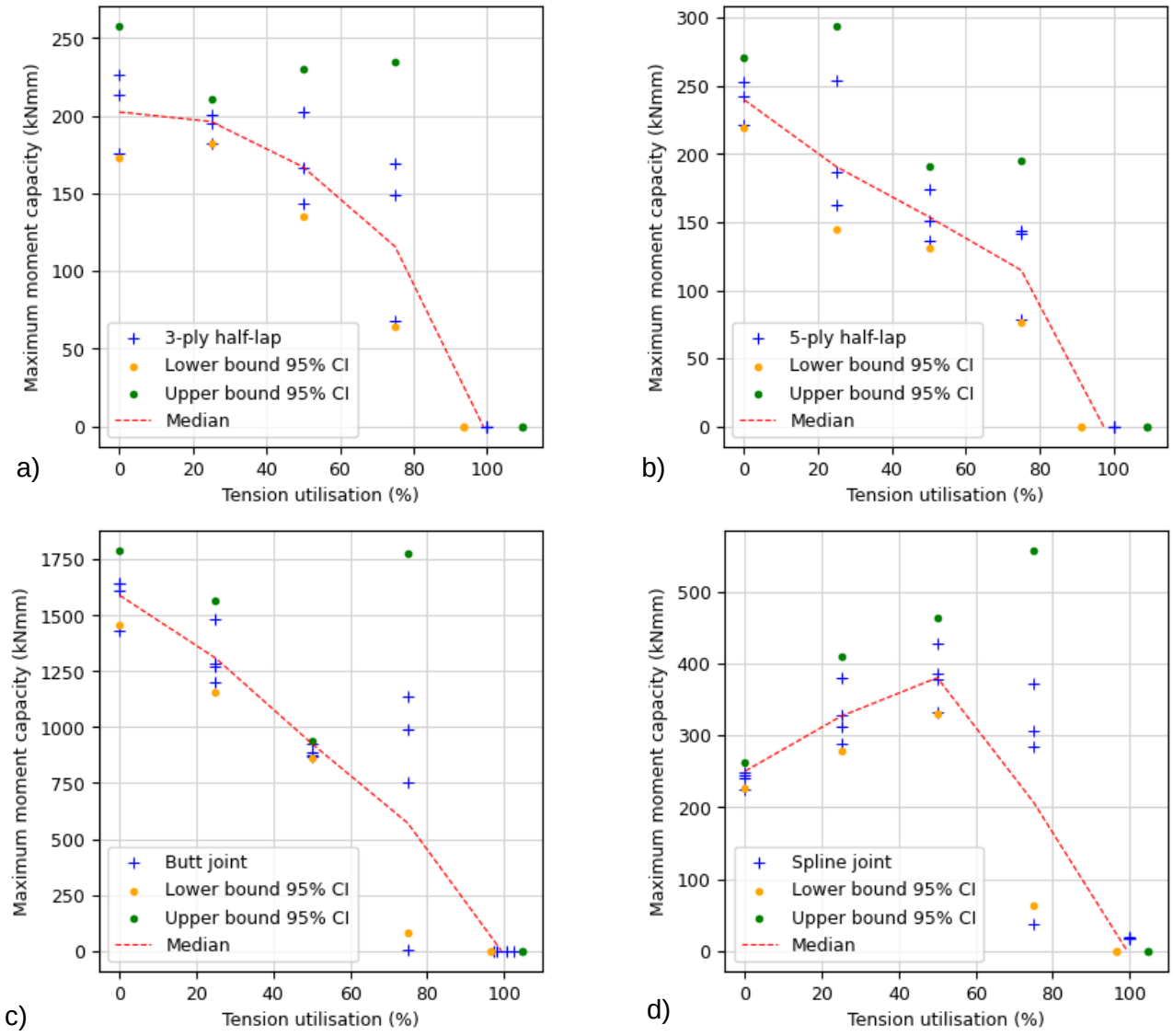

Figure 7: Force interaction curves from Setup A: 3-ply (a), 5-ply (b) half lap joint and Setup B: butt joint (c) and spline joint (d)

Looking at the rotation capacity interaction curves, 5-ply half lap (Figure 8b), butt joint (Figure 8c) and spline joint (Figure 8d) show significant increase until 25% and subsequent drop off, with spline having by far the largest increase. The 3-ply (Figure 8a) is an outlier here and it is also thought to be due to the difference in the failure modes.

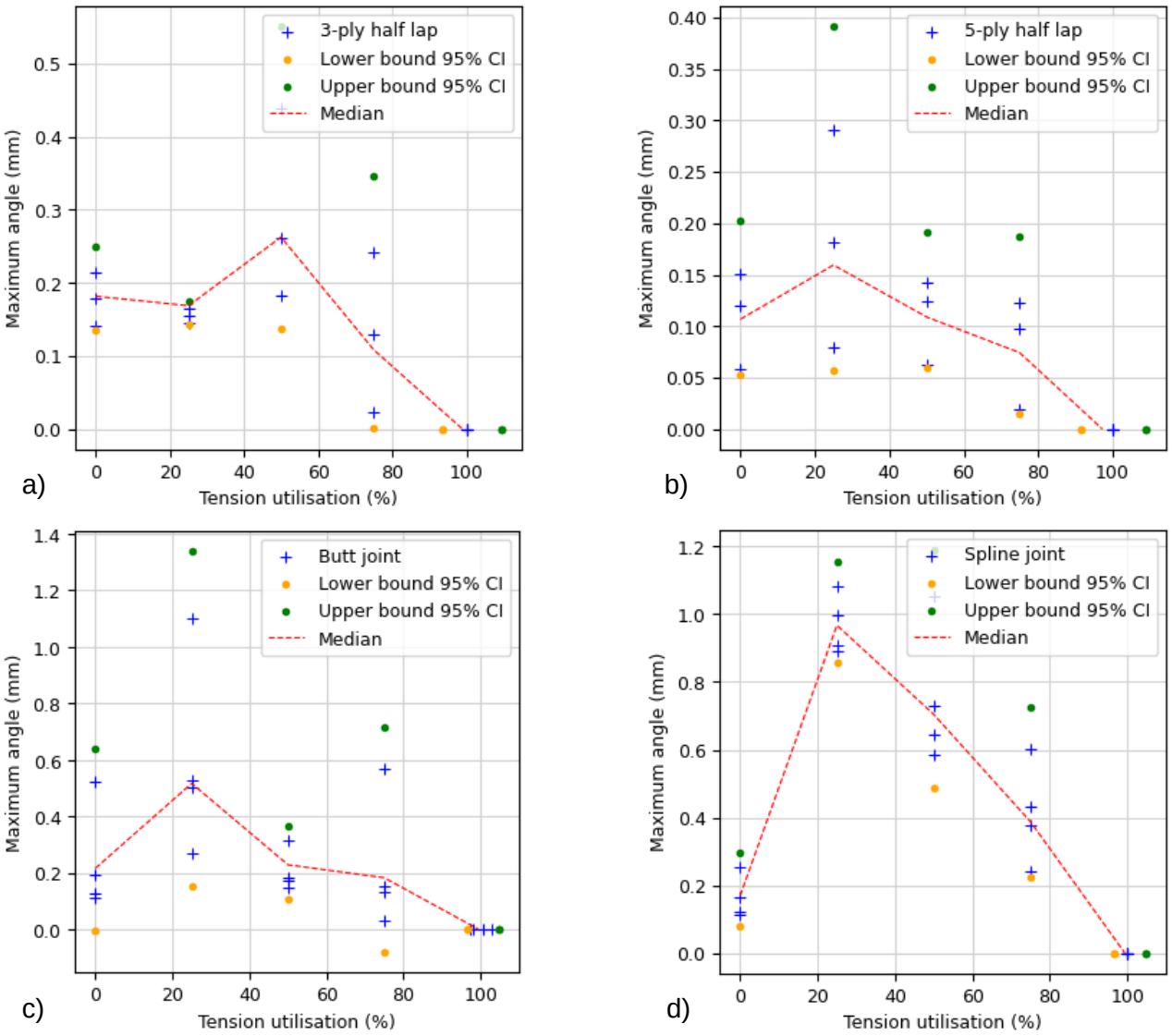

Figure 8: Rotation failure envelope curves from Setup A: 3-ply (a), 5-ply (b) half lap joint and Setup B: butt joint (c) and spline joint (d)

2.4.2 Full span test results

The component tests used active tensioning to a load level and subsequent vertical load pushdown. In true catenary action, this tension will gradually increase throughout the movement progression. The full-span tests aimed to evaluate the impact of combination of loading, progressively increasing the tension versus sustaining the same level of load throughout.

The load profiles of the full-span load hold samples and passive tension samples are compared in Figure 9. Both load hold and passive tension yielded comparable combination of vertical and horizontal forces at failure. However, it is noteworthy that load hold exhibited significantly higher variability and, in outlier cases, facilitated substantially larger deformations and loads. Therefore, when interpreting load hold results for the absolute characterisation of individual connection performance, it is important to exercise caution. However, given the general replicability of load combinations, the

load hold scenario can be effectively employed as a tool for introducing controlled parameters to investigate their influence on the behaviour of the connections, as was done in this study. This is crucial for advancing the more general understanding of connection behaviour and its underlying mechanisms.

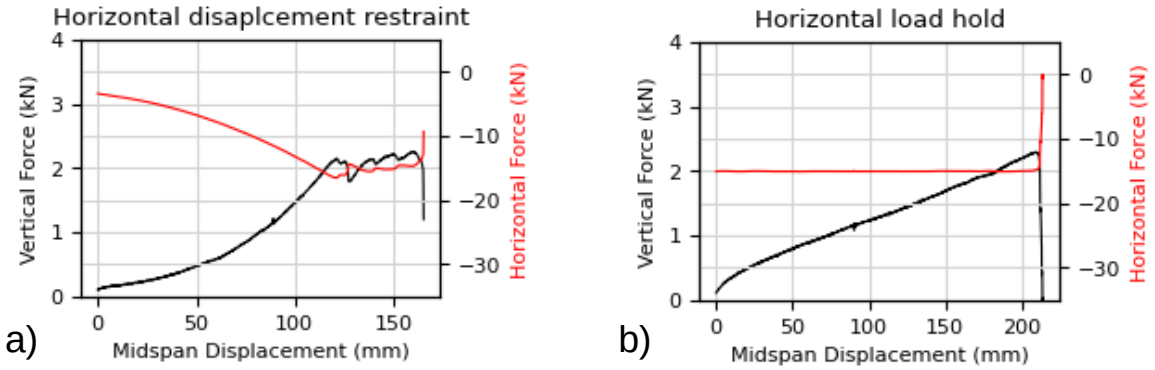

Figure 9: Load profiles of passive (a) and active (b) load induced catenary activation

The subsequent relative correlation between the tests at the two scales shown in Figure 10: Correlation between the component and full-span test. The 95% CI were developed by utilising the method of least squares on the CI values for each separate test type calculated through EV1, as shown before in Figure 7c. The full-span tests for the butt joint showed a decline in moment capacity proportional to increase in tension. Moreover, mapping both test types onto one another shows a good match, and although some of the full-span tests showcase a higher moment resistance, the lower confidence interval does a good job of capturing the bottom boundary of large-scale test values, which is the more crucial for design.

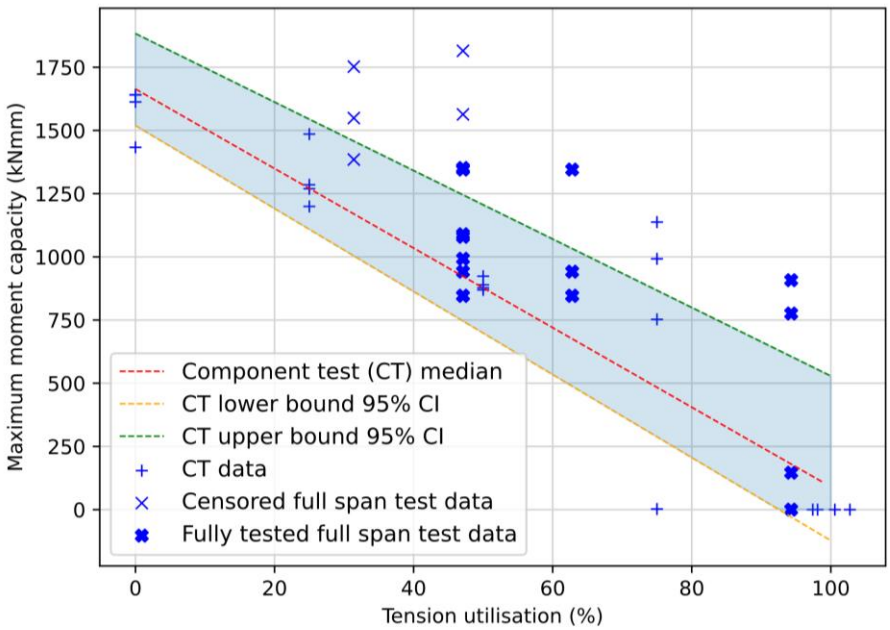

Figure 10: Correlation between the component and full-span test

2.4.3 Resultant butt joint tension within the connections

The internal resultant tension forces in the connector were calculated according to Equation (3) for the butt joint component tests. The tension present in the connection is a combination of the moment couple present from the opening of the joint and the external tension from catenary forces. For most of the tension utilisation levels the maximum tension force as well as the relating deflection corresponds to the uniaxial tension tests, as shown in Figure 11.

Despite different bi-axial load combinations this can therefore be used as a reliable parameter for failure checks. The overall shape of the curves also remains unchanged when compared to uniaxial tension tests. One of the most notable observations is that a positive correlation between the ability to progress through the post peak plateau within the connection, as seen in the 25% series and to limited extend in the 50%, which resulted in much higher overall force and deformation capacity (Figure 12:).

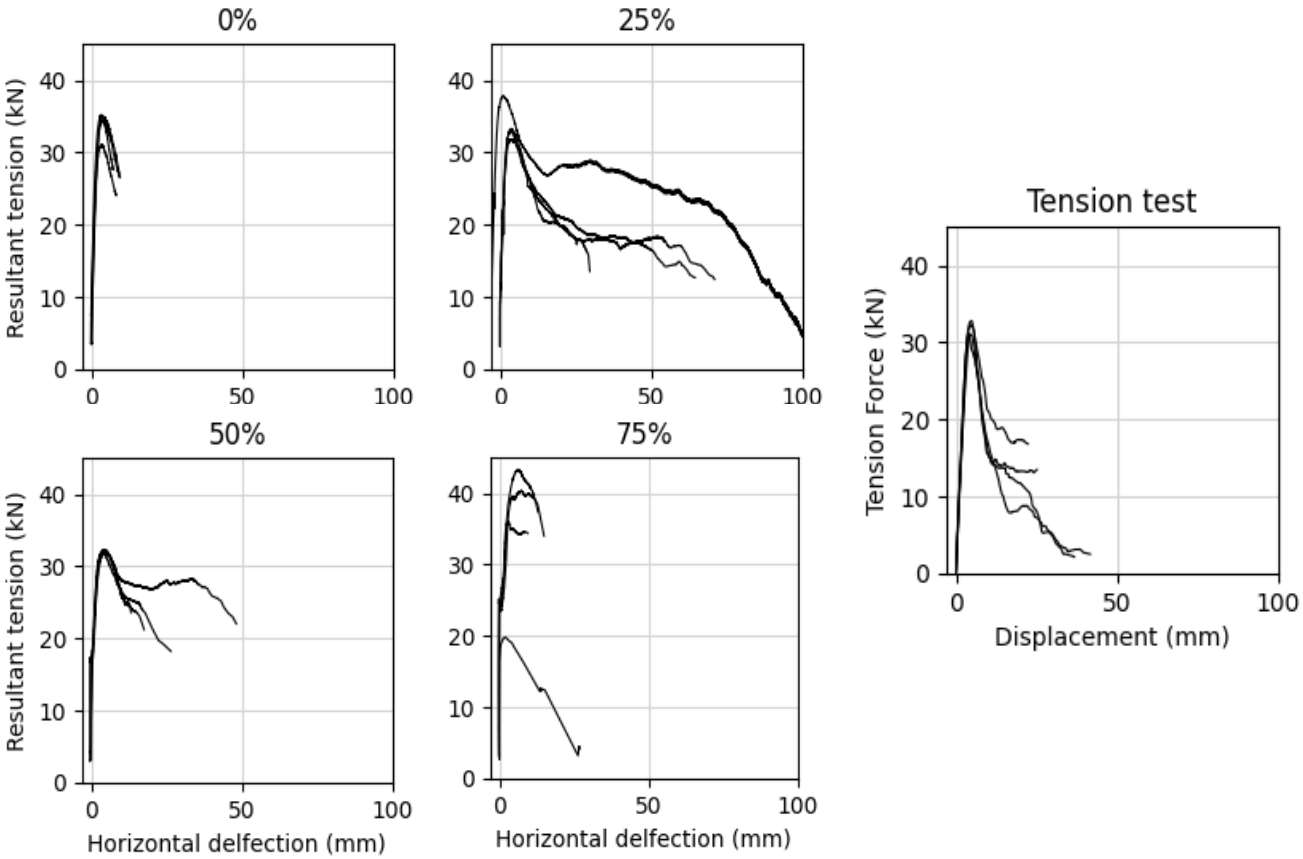

Figure 11: Resultant total tension at the screws in butt joint component tests as compared to the uniaxial tension test results

3 Numerical investigations

3.1 Overview

Numerical investigations were used to evaluate whether utilising experimental findings from the small-scale series (component combined tests and uniaxial tension tests) allow to predict the behaviours of the larger subassemblies. The model relies on empirically derived stiffness values of connections and is validated with the experimental results from the large-scale tests. The validated opens up the possibility for extensive parametric explorations concerning a wide range of subassembly geometries and other influential factors, such as the effects of support conditions on failure modes.

The model was built in the ABAQUS software utilising 2D beam elements and assigning them the cross-sectional properties of the CLT as used in the large-scale tests: 600 mm wide and 100 mm thick. The model focused on the butt joint, as it was investigated with most replicates in large scale testing and therefore the modelling results can be compared to the largest experimental database.

3.2 Spring model

The main challenge of accurate modelling is reconciling the interactions that the parameters have on one another, mainly the rotational spring stiffness. This stiffness under combined loading is nonlinear; its value along with maximum moment capacity varies with change in the tension utilisation T_u. This change is illustrated in Figure 12, which shows a comparison between force displacement and moment rotation curves of tests representative of their series.

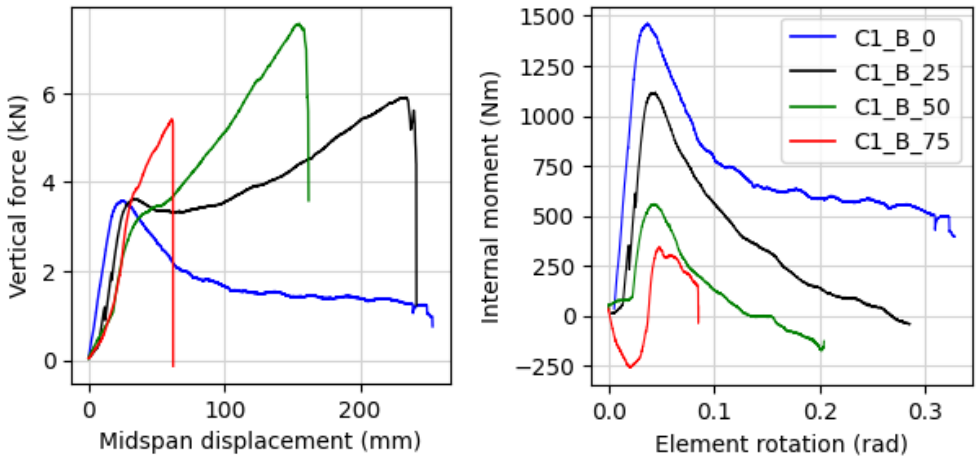

Figure 12: Vertical force displacement curve (a) and moment rotation curve (b) of the component tests at T_u of 0, 25, 50 and 75%

This parametric change required developing the two spring models shown in Figure 13. The axial stiffness of the fastener and the maximum tension force remain unchanged regardless of the overall maximum tension imposed on the connection (c.f. section 2.4.3). Thus, modelling the axial spring along with compressive point at a lever arm

seen in the connection (Figure 13a), result in a model that inherently accounts for rotational stiffness changes and could be used in all tension loading history cases. Figure 13b shows the more classic representation of connection behaviour, where the rotation and axial behaviour are treated as separate parameters. Its benefit is the simplicity, not requiring modelling a contact point, however it is only representative of a scenario under specified tension, which is uncommon in real catenary activation. Both were used in the following analysis to investigate their applicability.

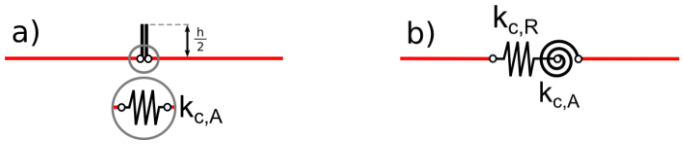

Figure 13: Connection spring models: a) axial spring with lever arm; b) series of rotational and axial non-dimensional spring

3.3 Results

Modelling the geometry and loading conditions of the larger setups can be predicted using the stiffness specification of the connector directly from the processed component test data, as shown in Figure 14. Both models a) and b) closely represent the test data, with model a) – the lever armed axial spring – showing higher stiffness and model b) – series of rotational and axial spring – showing lower stiffness. The governing failure criterion for model a) was reaching the ultimate tension force of the axial spring and for model b) it was the maximum rotation based on the values presented in Figure 8c).

Both models very closely predict the displacement under gravity loading. Model b) initially provides better results, with the stiffness accuracy dropping off with the increase of mid-span displacement. The failure point in model b) also better align with the experimental data. For model a), the idealised lever arm results in a higher stiffness which results in underestimation of the strength. In reality, the top contact point formation in failed specimen has consistently shown a contact slip or approx. 10 mm. Therefore, an empirical factor for lever arm of 0.8 was introduced to account for that, resulting in adjusted model a*). This adjustment allowed for a much better, however still conservative, prediction of the failure point and system stiffness.

The rotational spring model could also be improved for use under variable tension, which could be done through introducing parametric variables into the model. This however introduces another level of complexity and time cost, which might not be replicable in a lot of the design scenarios. The discrepancies in both models are attributed to the non-linearity of stiffnesses, however the linear approximations used along with the outlined failure criteria are thought to be sufficiently good predictors of the behaviour.

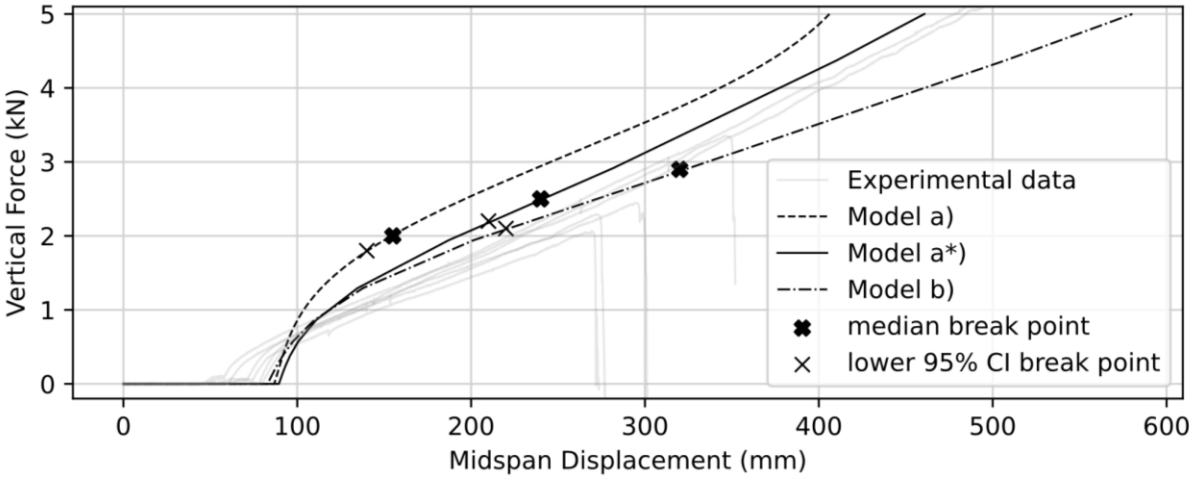

Figure 14: Comparison of ABAQUS and test results for a 15kN load hold

4 Conclusions

Moment-tension as well as maximum rotation-tension interaction curves were derived for 3 types of typically used CLT joints. For joints with significant rotational stiffness, a negative correlation was shown between the tension level and moment capacity. Supplementary rotation curves indicated that the best catenary can be achieved for most joints with around 25% of tension utilisation (normalised to maximum uniaxial tension). The spline connection exhibited the greatest benefit from catenary action; however, it did not offer significant bending stiffness in normal conditions.

A positive correlation was found between the full span test results of active load hold application and horizontal restraint methods. As these represent two extremes of boundary stiffness resulting in very different tension history, it can be asserted that given the same final force combinations, similar failure is to be expected irrespective of the loading history. This allows for a higher flexibility in methods of testing. Moreover, using component-level bending and tensile test results as input for numerical modelling has proven to be a dependable technique for predicting the behaviour of CLT floor subassemblies subjected to catenary action.

The emphasis on performance-based progressive collapse prevention holds significant importance for the future generation of timber design standards. The research presented herein provides an empirical foundation and presents an economical test approach, known as the component test method, for effectively measuring these parameters in connections.

References

Abrahamsen, R. (2017). Mjøstårnet-Construction of an 81 m tall timber building. Internationales Holzbau-Forum IHF, 12.

European Committee for Standardization. (2006). Eurocode 1 - Actions on structures - Part 1-7: General actions - Accidental actions BS EN 1991-1-7:2006 (Vol. 1, p. 66).

Gumbel, E. J. (1948). Statistical theory of extreme values and some practical applications: a series of lectures.: Vol. Vol. 33. US Government Printing Office.

Lyu, C. H., Gilbert, B. P., Guan, H., Underhill, I. D., Gunalan, S., Karampour, H., & Masaeli, M. (2020). Experimental collapse response of post-and-beam mass timber frames under a quasi-static column removal scenario. Engineering Structures, 213, 110562. https://doi.org/10.1016/j.engstruct.2020.110562

Mpidi Bita, H., & Tannert, T. (2019). Experimental Study of Disproportionate Collapse Prevention Mechanisms for Mass-Timber Floor Systems. Journal of Structural Engineering, 146(2), 04019199. https://doi.org/10.1061/(ASCE)ST.1943-541X.0002485

Starossek, U., & Haberland, M. (2012). Robustness of structures. Int. J. Lifecycle Performance Engineering, 1(1), 3–21. https://doi.org/10.1504/IJLCPE.2012.051279

Voulpiotis, K., Köhler, J., Jockwer, R., & Frangi, A. (2021). A holistic framework for designing for structural robustness in tall timber buildings. Engineering Structures, 227, 111432. https://doi.org/10.1016/j.engstruct.2020.111432